

Research Article

Development for High-Accuracy *In Vitro* Assay of Vascular Endothelial Growth Factor Using Nanomagnetically Labeled Immunoassay

C. C. Yang,¹ K. W. Huang,^{2,3} S. Y. Yang,^{1,4} H. H. Chen,⁴ T. C. Chen,¹ C. S. Ho,¹ S. F. Chang,¹ J. J. Chieh,⁴ H. E. Horng,⁴ C. Y. Hong,⁵ and H. C. Yang⁶

¹ MagQu Co., Ltd., Xindian District, New Taipei City 231, Taiwan

² Department of Surgery & Hepatitis Research Center, National Taiwan University Hospital, Taipei 100, Taiwan

³ Graduate Institute of Clinical Medicine, College of Medicine, National Taiwan University, Taipei 100, Taiwan

⁴ Institute of Electro-Optical Science and Technology, National Taiwan Normal University, Taipei 116, Taiwan

⁵ Graduate Institute of Biomedical Engineering, National Chung Hsing University, Taichung 402, Taiwan

⁶ Department of Electro-Optical Engineering, Kun Shan University, Yongkang District, Tainan City 710, Taiwan

Correspondence should be addressed to S. Y. Yang; syyang@magqu.com and H. E. Horng; phyfv001@ntnu.edu.tw

Received 25 February 2013; Revised 24 August 2013; Accepted 26 August 2013

Academic Editor: Oleg Petravic

Copyright © 2013 C. C. Yang et al. This is an open access article distributed under the Creative Commons Attribution License, which permits unrestricted use, distribution, and reproduction in any medium, provided the original work is properly cited.

Nanomagnetically labeled immunoassays have been demonstrated to be promisingly applied in clinical diagnosis. In this work, by using antibody-functionalized magnetic nanoparticles and a high-temperature superconducting quantum interference device as magnetosusceptometer, the assay properties for vascular endothelial growth factor (VEGF) in serum are investigated. By utilizing the assay method so-called immunomagnetic reduction, the properties of assaying VEGF are explored. In addition, the VEGF concentrations in serum samples of normal people and patients with either colorectal or hepatocellular cancer are detected. The experimental results show that the low-detection limit for assaying VEGF is 10 pg/mL, which is much lower than the clinical cut-off VEGF concentration of 50 pg/mL for diagnosing malignancy. Besides, there are no significant interference effects on assaying VEGF from hemoglobin, conjugated bilirubin, and triglyceride. The VEGF concentrations in serum samples donated by normal people and patients with hepatocellular carcinoma or colorectal cancer are detected. A clear difference in VEGF concentrations between these two groups is found. These results reveal the feasibility of applying nanomagnetically labeled immunoassay to clinics.

1. Introduction

Early-stage diagnosis is the trend for *in vitro* diagnosis. For immunoassay, the important requirements with early-stage diagnosis are the abilities to assay the ultra-low-concentration biomarkers. One of the categories in the early-stage immunoassay is the screening of malignancy. The biomarker for malignancy is vascular endothelial growth factor (VEGF) [1–4]. In clinics, the cut-off concentration for VEGF is 50 pg/mL. This means the VEGF concentration in the noncancer population is lower than 50 pg/mL [5, 6]. Thus, the low-detection limit of assay kits for VEGF would be better to be lower than 5 pg/mL, or even down to sub-pg/mL.

One popular method to assay VEGF is the so-called enzyme-linked immunosorbent assay (ELISA) [7–9]. However, it is difficult to detect VEGF at low concentrations, such as tens of pg/mL, using ELISA. Further, it requires much time and skill. The results from ELISA tend to be confounded by hemolysis or jaundice, and these phenomena are very common in the blood of cancer patients [10]. Hence, ELISA is usually used to diagnose mild to serve malignancy, not for early-stage diagnosis.

Some of the coauthors developed assay technologies for quantitatively detecting ultra-low-concentration biomolecules [11, 12]. This technology is referred to as SQUID-based immunomagnetic reduction (IMR), where SQUID is

the abbreviation for superconducting quantum interference device. It was demonstrated that the low-detection limit of SQUID-based IMR to assay β -amyloids is around pg/mL [13, 14]. Thus, it can hopefully be applied to SQUID-based IMR for the quantitative detection of ultra-low-concentration VEGF. This motivates us to characterize the assay of VEGF using SQUID-based IMR.

The detailed physical mechanism of IMR is reported in [15]. Instead of tedious theoretical discussion, phenomenological explanations for IMR are given here. IMR is such a method as assaying target molecules via measuring the reduction in the mixed-frequency magnetic susceptibility of the magnetic reagent owing to the association between magnetic nanoparticles and target molecules, as illustrated in Figures 1(a) and 1(b). Under external multiple ac magnetic fields, magnetic nanoparticles oscillate with the multiple ac magnetic fields via magnetic interaction. Thus, the reagent under external multiple ac magnetic fields shows a magnetic property, called mixed-frequency ac magnetic susceptibility χ_{ac} , as illustrated in Figure 1(a). Via the antibodies on the outmost shell, magnetic nanoparticles associate with and magnetically label biotargets. With the association, magnetic nanoparticles become larger or clustered, as schematically shown in Figure 1(b). The response of these larger magnetic nanoparticles to external multiple ac magnetic fields becomes much less than that of originally individual magnetic nanoparticles. Thus, the χ_{ac} of the magnetic reagent is reduced due to the association between magnetic nanoparticles and biotargets. In principle, as the amounts of biotargets are reduced, fewer magnetic nanoparticles become larger or clustered. The reduction in χ_{ac} of the reagent is depressed. Once the reduction in χ_{ac} is depressed to be lower than the noises of χ_{ac} of the reagent, the assay result becomes negative. To achieve highly sensitive detections, it is preferred to utilize a detection module with low noise and high sensitivity to χ_{ac} signals. This is why SQUID is used for IMR because it is a more sensitive sensor of magnetic signals.

In this work, SQUID-based IMR is applied to explore the low-detection limit for assaying VEGF. In addition, the interferences by several materials such as hemoglobin, bilirubin, and triglyceride to the assays of VEGF are investigated for SQUID-based IMR. These results are compared with those done via ELISA. Finally, the VEGF concentrations in human serum from patients with hepatocellular carcinoma or colorectal cancer, as well as normal people, are detected using SQUID-based IMR.

2. Materials and Methods

The magnetic reagent used here is magnetic nanoparticles, which are biofunctionalized with antibodies against VEGF (anti-VEGF), and dispersed in pH 7.4 phosphate buffered saline solution (MF-VEG-0060, MagQu). The magnetic core of the particles is Fe_3O_4 . The Fe_3O_4 cores are individually enveloped with dextran. The size distribution of dextran-coated Fe_3O_4 particles was detected by dynamic laser scattering (Nanotracer-150, Microtrac). The results are shown in Figure 2(a). The mean diameter was found to be 49.7 nm.

Through chemical reactions, anti-VEGF is covalently bound with dextran [16, 17]. By using dynamic laser scattering (Nanotracer-150, Microtrac), the diameter distribution of the biofunctional magnetic nanoparticles was measured, as shown in Figure 2(b). The mean diameter of the biofunctionalized Fe_3O_4 nanoparticles is 57.2 nm. The stability of magnetic reagent stored at 2–8°C is examined by analyzing the time-evolution mean value of the hydrodynamic diameter of particles. The results are shown in Figure 3 and reveal that the hydrodynamic diameter of particles remains unchanged for 36 weeks. This implies that there is no agglomeration of particles in the reagent stored at 2–8°C for 36 weeks. The magnetic hysteresis curve of the magnetic reagent was measured with a vibrating sample magnetometer (HyterMag, MagQu), as shown in Figure 4. The saturated magnetization of the magnetic reagent is 0.3 emu/g, corresponding to the particle concentration of 10^{12} particles/mL. Besides, the magnetic reagent shows superparamagnetism.

60 μL magnetic reagent was thoroughly mixed with the 60 μL sample solution in a glass tube. The χ_{ac} signal, $\chi_{ac,o}$, of the mixture before the formation of immunocomplex of VEGF-magnetic-nanoparticles was recorded using a magnetic immunoassay analyzer (XacPro-S, MagQu). Then, the mixture was kept at room temperature for the formation of VEGF-magnetic-nanoparticles, followed by recording the χ_{ac} signal, $\chi_{ac,\phi}$, of the mixture. It usually takes 3 hours for finishing the formation of VEGF-magnetic-nanoparticles. With the measured $\chi_{ac,o}$ and $\chi_{ac,\phi}$, the IMR signal can be obtained via

$$\text{IMR (\%)} = \frac{(\chi_{ac,o} - \chi_{ac,\phi})}{\chi_{ac,o}} \times 100\%. \quad (1)$$

For a given sample solution, the sample was divided into three parts for the triple tests of IMR signals. With the three individual IMR signals, the mean value and the standard deviation of the IMR signals were calculated. To build the characteristic curve, that is, the relationship between the IMR signal and VEGF concentration, various amounts of VEGF (PEP400-31-10, PeproTech) were added to the PBS solution, followed by measuring the IMR signals for these VEGF solutions.

As to the human serum, the $\chi_{ac,o}$ and $\chi_{ac,\phi}$ of the mixture of 60 μL serum and 60 μL magnetic reagent were detected using a magnetic immunoassay analyzer (XacPro-S, MagQu). Thus, the IMR signals can be obtained via (1) for human serum.

VEGF levels were detected using the Quantikine Human VEGF-ELISA kit (R&D Systems, Minneapolis, MN) [18]. 100 μL of rat serum and serially diluted standard solutions (VEGF) were added to 96-well microtiter plates precoated with murine anti-VEGF monoclonal antibodies and incubated at room temperature for 2 hours. After incubation, 200 μL of the secondary antibody, an enzyme-linked EGF-specific polyclonal goat antibody, was added, and then, incubation continued for 2 hours at room temperature. Substrate solution was added, and the reaction continued for 30 minutes. The optical density at a 450 nm wavelength is detected with an ELSIA reader.

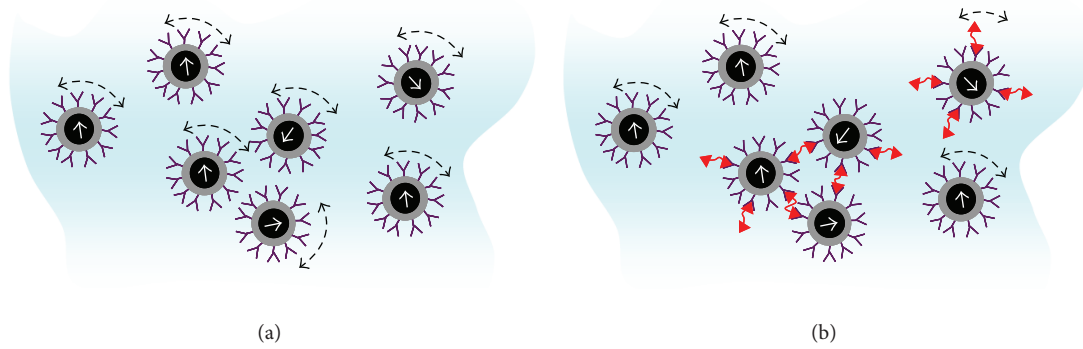


FIGURE 1: Illustration of the mechanism of immunomagnetic reduction (IMR).

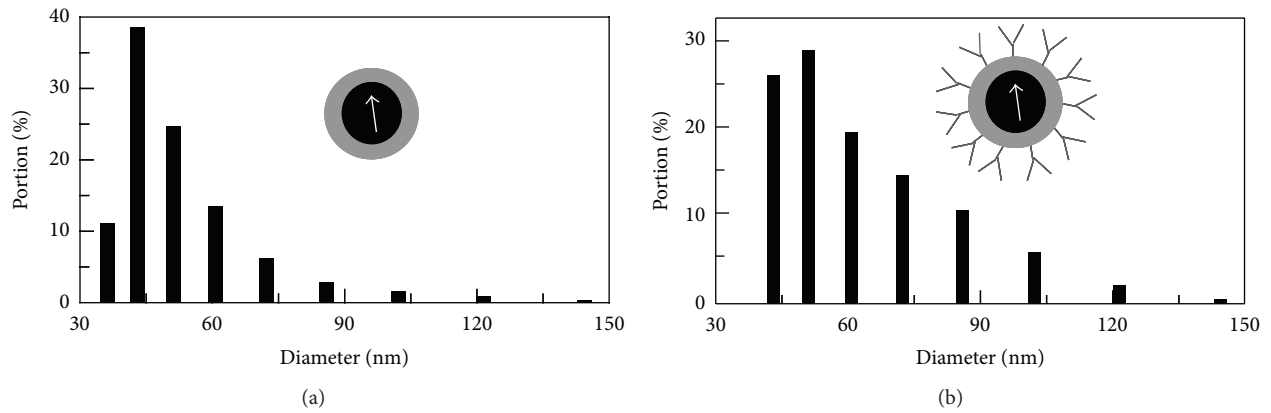
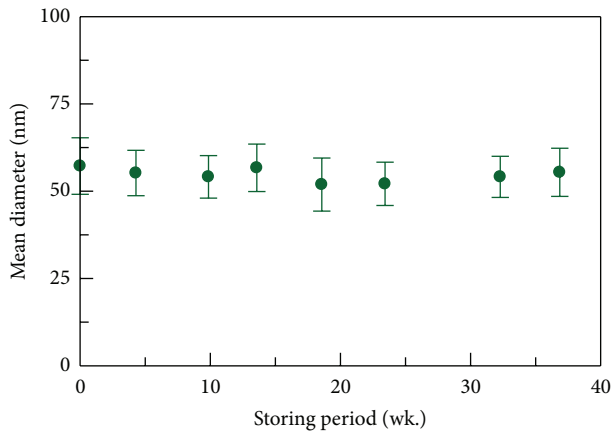
FIGURE 2: Distribution analysis for the hydrodynamic diameters of (a) dextran-coated Fe_3O_4 nanoparticles and (b) anti-VEGF functionalized Fe_3O_4 nanoparticles dispersed in PBS solution.

FIGURE 3: Time-evolution mean diameter of magnetic particles biofunctionalized with anti-VEGF and dispersed in PBS solution.

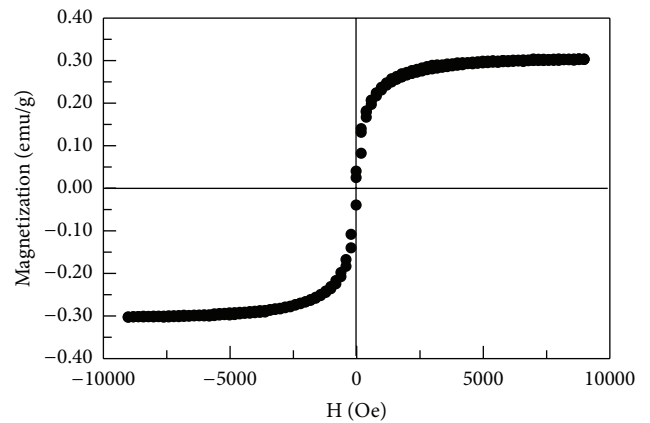


FIGURE 4: Magnetic hysteresis curve of magnetic nanoparticles functionalized with anti-VEGF and dispersed in PBS solution.

3. Results and Discussion

The optical density (OD) as a function of the VEGF concentration detected via ELISA was characterized, as shown with the crosses and the dashed line in Figure 5. The error

bars are the standard deviations of the triple-test signals. It was found that OD almost remains constant as VEGF concentration ϕ_{VEGF} increases from 1 pg/mL to 23.4 pg/mL. As VEGF concentration ϕ_{VEGF} is higher than 46.9 pg/mL, a significant increase in OD is observed. The low-detection

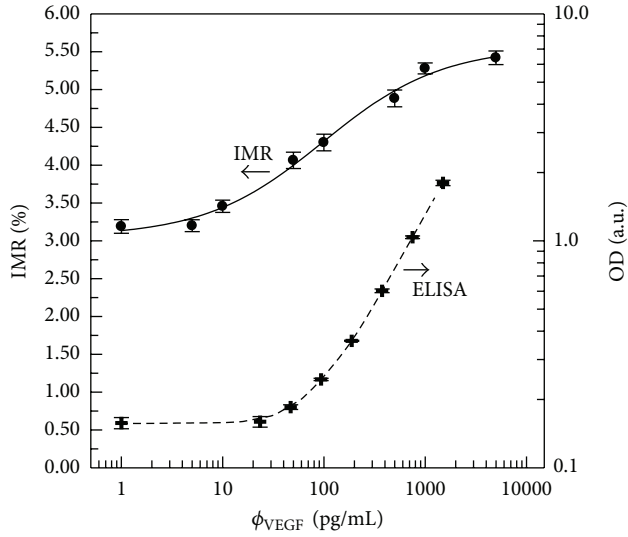


FIGURE 5: VEGF concentration dependent IMR signals (dots with the solid line) using immunomagnetic reduction (IMR) and OD (crosses with the dashed line) using ELISA.

limit in OD can be obtained by the addition of triple standard deviations (e.g., 3-sigma criterion) to the OD at low VEGF concentrations. The OD at 23.4 pg/mL VEGF is 0.160, and its standard deviation is 0.009. The low-detection limit in OD is $(0.160 + 3 \times 0.009)\% = 0.187\%$, which is very close to the OD at 46.9 pg/mL VEGF, that is, 0.185. This implies that the low-detection limit for assaying VEGF via ELISA is around 50 pg/mL. However, the cut-off concentration for VEGF in clinics is 50 pg/mL. The results shown by the dashed line in Figure 3 reveal that the ELISA is not sensitive enough to assay VEGF for patients in early-stage malignancy.

SQUID-based IMR is applied to characterize the VEGF concentration dependent IMR signals. The results are shown by the dots in Figure 5. The error bar at each VEGF concentration is the standard deviation of the triple-test IMR signals. Clearly, there is no difference in IMR signals ($\sim 3.2\%$) for ϕ_{VEGF} being 1 and 5 pg/mL. For ϕ_{VEGF} being 10 pg/mL, the IMR signal ($\sim 3.5\%$) definitely deviates from that of ϕ_{VEGF} being 1 or 5 pg/mL. The low-detection limit in IMR signals can be obtained by adding triple standard deviations (e.g. 3-sigma criterion) to the IMR signals at low VEGF concentrations. According to Figure 5, the IMR signal at 5 pg/mL VEGF is 3.20%, and its standard deviation is 0.08%. The low-detection limit in IMR signal turns to $(3.20 + 3 \times 0.08)\% = 3.44\%$, which is slightly lower than the IMR signal at 10 pg/mL VEGF, that is, 3.46%. Therefore, the low-detection limit for assaying VEGF using SQUID-based IMR is 10 pg/mL, which is lower than the clinical cut-off VEGF concentration 50 pg/mL. Hence, SQUID-based IMR would be good for early-stage diagnosis of malignancy.

As the VEGF concentration keeps increasing from 10 pg/mL, the IMR signal also increases and becomes saturated as the VEGF concentration is over 1000 pg/mL.

The VEGF concentration dependent IMR signals in Figure 3 exhibit such behavior of logistic function. Consider

$$\text{IMR}(\%) = \frac{A - B}{1 + (\phi_{\text{VEGF}}/\phi_o)^\gamma} + B, \quad (2)$$

where A , B , ϕ_o , and γ are fitting parameters. By fitting dots in Figure 3 to (2), A was found to be 3.05, B was 5.56, ϕ_o equaled 98.84, and γ was 0.74. The fitting curve of (2) is plotted by the solid curve in Figure 5. The coefficient of determination R^2 between the dots and the solid line is 0.993, denoting a high consistency between the experimental data (dots) and the fitting curve (solid line).

Note, the value of A in (2) corresponds to the IMR signal at zero VEGF concentration. Theoretically, the value of A should be zero. However, due to noises in the mixed-frequency ac magnetic susceptibility χ_{ac} , a nonzero IMR signal is resulted, even if there is no VEGF molecules in the tested sample. Hence, the value of A in (2) is not zero. The noises are attributed from two main factors. One factor is the electric noise generated by the immunoanalyzer. The other factor is referred to as bioreaction noise, which results from the dynamic balance of the association/dissociation between VEGF molecules and anti-VEGF functionalized magnetic nanoparticles.

For serum, there might be interfering materials due to hemolysis, jaundice, or hypertriglyceridemia, such as hemoglobin (Hb), conjugated bilirubin (C-BL), or triglyceride (TG). It is necessary to clarify the interference effects of these materials on assaying VEGF. Besides, biomarkers for other cancers like hepatocellular carcinoma (HCC) or colorectal cancer (CRC) are included for the interference tests. In clinics, the biomarker for HCC is alpha-fetoprotein (AFP), while carcinoembryonic antigen (CEA) is the biomarker for CRC. The cut-off concentrations for these interfering materials are listed in Table 1. When someone's serum contains a certain biomarker concentration exceeding its cut-off value, he or she is suffering from the corresponding disease. For example, if someone's serum contains Hb higher than 500 $\mu\text{g/mL}$, say 600 $\mu\text{g/mL}$, he or she is suffering from hemolysis. Table 1 shows that the concentrations of these interfering materials used for the interference tests are much higher than the cut-off concentrations. For comparison, the interference tests for VEGF were done using ELISA and IMR, respectively.

The 100 pg/mL VEGF solutions without or with interfering materials are used as test samples. The optical densities (OD) for these solutions are detected using ELISA and are plotted in Figure 6(a). The data of these ODs are listed in Table 2. In the experiment, the sample without interfering material (labeled with "None" in Figure 6(a)) is used as a reference. The OD of the reference sample was observed to be 0.31 ± 0.01 . The samples with 1000 $\mu\text{g/mL}$ Hb, 10 $\mu\text{g/mL}$ C-BL, and 2000 $\mu\text{g/mL}$ TG show distinctly higher OD's as compared to that of the reference sample, while the sample with 100 ng/mL AFP shows differentially lower OD. These results reveal the significant interference by biomolecules of Hb, C-BL, TG, and AFP for assaying VEGF using ELISA.

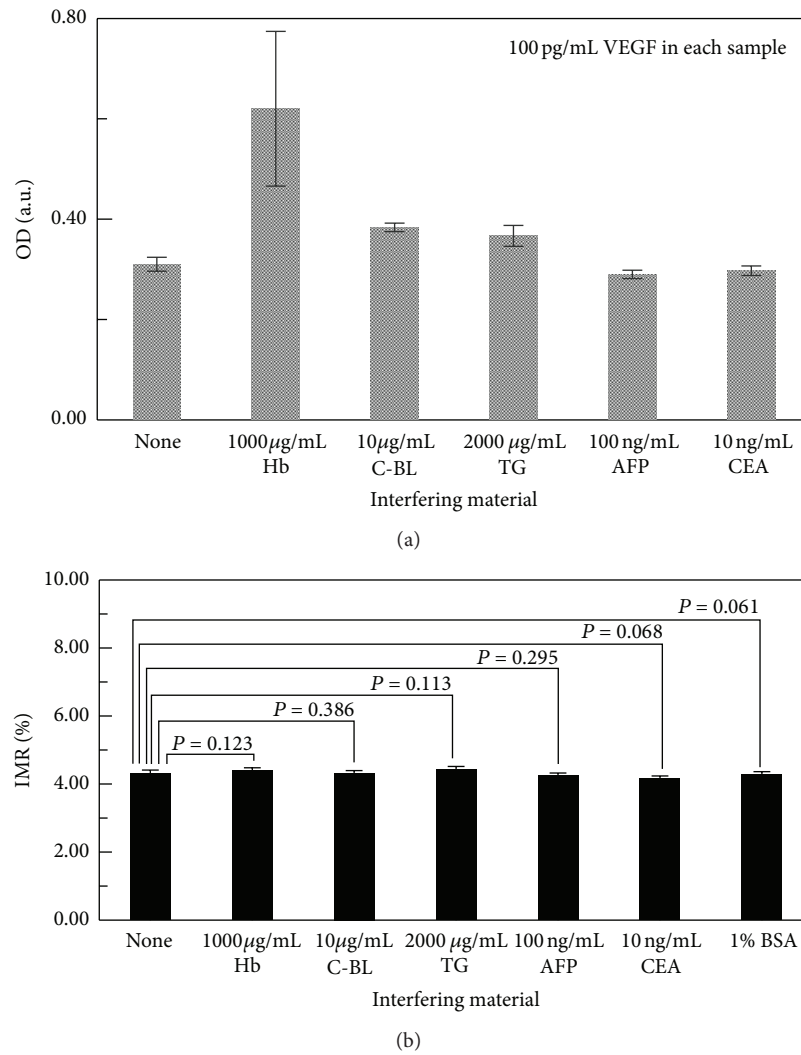


FIGURE 6: Interference tests for (a) ELISA and (b) IMR by interfering materials such as Hb, C-BL, TG, AFP, and CEA.

TABLE 1: Clinical cut-off concentrations and used concentrations in this work for interference tests due to hemoglobin (Hb), conjugated bilirubin (C-BL), triglyceride (TG), alpha-fetoprotein (AFP), and carcinoembryonic antigen (CEA).

Disease	Hemolysis	Jaundice	Hypertriglyceridemia	Hepatocellular carcinoma	Colorectal cancer
Biomarker (as interfering material)	Hb	C-BL	TG	AFP	CEA
Cut-off concentration	500 µg/mL	2 µg/mL	1500 µg/mL	20 ng/mL	5 ng/mL
Concentration used for interference test	1000 µg/mL	10 µg/mL	2000 µg/mL	100 ng/mL	10 ng/mL

As to the interference tests for IMR, the IMR signals for these VEGF solutions without or with interfering materials are detected and shown in Figure 6(b). One more interfering material, 1% bovine serum albumin (BSA), is used for the interference tests for IMR. The IMR signal for the reference sample, which consists of pure 100 pg/mL VEGF, was found to be $(4.30 \pm 0.11)\%$. The IMR signals of the other samples with interfering materials are listed in Table 2. There is hardly any difference in IMR signals between the samples with interfering material and the reference sample. A quantitative analysis of the consistency in IMR signals between samples with interfering materials and the reference sample was done

through *t*-test statistic analysis. A quantity, *P* value, was calculated for the consistency in IMR signals between samples with interfering materials and the reference sample, as labeled in Figure 6(b). It was found that all *P* values are higher than 0.05, meaning that there was no significant difference in IMR signals for VEGF solutions without interfering materials as compared to that of the pure VEGF solution.

In addition to the high specificity of antibodies against VEGF molecules, there are two important factors relevant to the high specificity in assaying VEGF using IMR. The first factor is that the signals detected using IMR are magnetic instead of optical for ELISA. The colors due to Hb, C-BL, or

TABLE 2: Experimental data of ODs and IMR signals for the interference tests using ELISA and IMR, respectively. The results are plotted in Figures 6(a) and 6(b).

Interfering material	None	Hb	C-BL	TG	AFP	CEA	BSA
OD	0.31 ± 0.01	0.62 ± 0.15	0.38 ± 0.008	0.37 ± 0.02	0.29 ± 0.008	0.29 ± 0.01	—
IMR signal (%)	4.30 ± 0.11	4.40 ± 0.07	4.32 ± 0.07	4.42 ± 0.10	4.26 ± 0.07	4.15 ± 0.09	4.28 ± 0.08

TG seriously affect the optical signals for ELISA but do nothing to with magnetic signals for IMR. The second factor is the suppression of nonspecific binding between antibodies and interfering molecules. Briefly speaking, the bound molecules with antibodies on magnetic particles experience centrifugal force because of the rotation of particles under external ac magnetic fields. The centrifugal force is enhanced under higher rotating frequencies. However, the binding force between anti-VEGF and non-specific molecules is weaker than that between anti-VEGF and specific molecules, that is, VEGF molecules. Thus, by suitably adjusting the frequencies of the external magnetic fields, the centrifugal force is strong enough to break out the binding between anti-VEGF and non-specific molecules but still weaker than the binding force between anti-VEGF and VEGF molecules. Therefore, the non-specific binding can be significantly depressed in IMR. Other examples for demonstrating the depression in the non-specific binding by adjusting the frequencies of the external magnetic fields are reported in [19].

With the relationship between the IMR signals and VEGF concentration, that is, $\text{IMR}(\%)-\phi_{\text{VEGF}}$ curve, in Figure 5, the VEGF concentrations ϕ_{VEGF} in human serum are detected using IMR. The serum can be categorized into three groups. The first group is sixteen serum samples from people without tumors, denoted as the normal group. The second group is sixteen serum samples from patients with HCC, referred to as the HCC group. The third group is sixteen serum samples of patients with CRC, referred to as the CRC group. The detected VEGF concentrations ϕ_{VEGF} using IMR for these forty-eight serum samples are shown in Figure 7. It was found that the ϕ_{VEGF} for normal group ranges from 9 to 40 pg/mL, which is well below the cut-off concentration in clinics of 50 pg/mL. However, for either the HCC group or CRC group, ϕ_{VEGF} is much higher than 50 pg/mL. A clear difference in the VEGF concentration in serum is obtained between the normal group and cancer (HCC and CRC) group using IMR.

4. Conclusions

By utilizing magnetic nanoparticles biofunctionalized with anti-VEGF and the SQUID-based mixed-frequency ac magnetosusceptometer, the assay properties for VEGF using immunomagnetic reduction (IMR) technologies are investigated. The SQUID-based IMR shows an ultra-low detection limit and nonsignificant interference for assaying VEGF. Further, there is a clear difference in the detected VEGF concentration in the serum between the normal group and the cancer group with hepatocellular carcinoma or colorectal cancer. These results demonstrate the feasibility of achieving clinically high sensitivity and high specificity for diagnosing

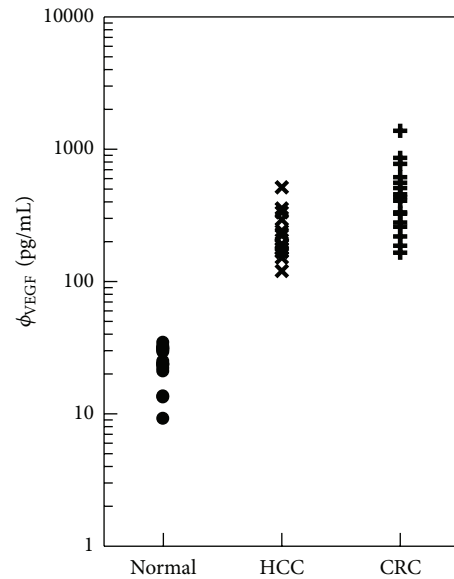


FIGURE 7: Detected VEGF concentrations in serum using SQUID-based IMR for normal people and patients with hepatocellular carcinoma (HCH) or colorectal cancer (CRC).

malignancy by assaying VEGF in serum using SQUID-based IMR.

Acknowledgments

This work was supported by the National Science Council of Taiwan under Grants nos. 102-2112-M-003-017, 102-2923-M-003-001, 102-2120-M-168-001, 102-2112-M-168-001, 102-2221-E-003-008-MY2, and 101-2221-E-003-005, the Department of Health under Grants nos. DOH101-TD-N-111-004, DOH100-TD-N-111-008, and DOH100-TD-PB-111-TM022, and the Ministry of Economic Affairs of Taiwan under Grants nos. 101-EC-17-A-17-II-0074, 1Z970688, and 1Z0990415 (SBIR).

References

- [1] G. Viglietto, D. Maglione, M. Rambaldi et al., "Upregulation of vascular endothelial growth factor (VEGF) and downregulation of placenta growth factor (PIGF) associated with malignancy in human thyroid tumors and cell lines," *Oncogene*, vol. 11, no. 8, pp. 1569–1579, 1995.
- [2] K. Podar and K. C. Anderson, "The pathophysiologic role of VEGF in hematologic malignancies: therapeutic implications," *Blood*, vol. 105, no. 4, pp. 1383–1395, 2005.
- [3] R. S. Finn and A. X. Zhu, "Targeting angiogenesis in hepatocellular carcinoma: focus on VEGF and bevacizumab," *Expert Review of Anticancer Therapy*, vol. 9, no. 4, pp. 503–509, 2009.

- [4] R. Bendardaf, A. Buhmeida, M. Hilska et al., "VEGF-1 expression in colorectal cancer is associated with disease localization, stage, and long-term disease-specific survival," *Anticancer Research*, vol. 28, no. 6 B, pp. 3865–3870, 2008.
- [5] I. Hyodo, T. Doi, H. Endo et al., "Clinical significance of plasma vascular endothelial growth factor in gastrointestinal cancer," *European Journal of Cancer*, vol. 34, no. 13, pp. 2041–2045, 1998.
- [6] K. Werther, I. J. Christensen, H. J. Nielsen et al., "Prognostic impact of matched preoperative plasma and serum VEGF in patients with primary colorectal carcinoma," *British Journal of Cancer*, vol. 86, no. 3, pp. 417–423, 2002.
- [7] F. M. Belgore, A. D. Blann, and G. Y. Lip, "Measurement of free and complexed soluble vascular endothelial growth factor receptor, Flt-1, in fluid samples: development and application of two new immunoassays," *Clinical Science*, vol. 100, no. 5, pp. 567–575, 2001.
- [8] S. Ponticelli, A. Braca, N. De Tommasi, and S. De Falco, "Competitive ELISA-based screening of plant derivatives for the inhibition of VEGF family members interaction with vascular endothelial growth factor receptor 1," *Planta Medica*, vol. 74, no. 4, pp. 401–406, 2008.
- [9] S. Greenberger, E. Boscolo, I. Adini, J. B. Mulliken, and J. Bischoff, "Corticosteroid suppression of VEGF-A in infantile hemangioma-derived stem cells," *The New England Journal of Medicine*, vol. 362, no. 11, pp. 1005–1013, 2010.
- [10] K. W. Huang, S. Y. Yang, Y. W. Hong et al., "Feasibility studies for assaying alpha-fetoprotein using antibody-activated magnetic nanoparticles," *International Journal of Nanomedicine*, vol. 7, pp. 1991–1996, 2012.
- [11] J. J. Chieh, S. Y. Yang, Z. F. Jian et al., "Hyper-high-sensitivity wash-free magnetoreduction assay on biomolecules using high- T_c superconducting quantum interference devices," *Journal of Applied Physics*, vol. 103, no. 1, Article ID 014703, pp. 1–6, 2008.
- [12] J. J. Chieh, S.-Y. Yang, H.-E. Horng et al., "Immunomagnetic reduction assay using high- T_c superconducting-quantum-interference-device-based magnetosusceptometry," *Journal of Applied Physics*, vol. 107, no. 7, Article ID 074903, pp. 1–5, 2010.
- [13] C. C. Yang, S. Y. Yang, J. J. Chieh et al., "Biofunctionalized magnetic nanoparticles for specifically detecting biomarkers of Alzheimer's Disease in vitro," *ACS Chemical Neuroscience*, vol. 2, pp. 500–505, 2011.
- [14] M. J. Chiu, H. E. Horng, J. J. Chieh et al., "Multi-channel squid-based ultra-high-sensitivity *in-vitro* detections for bio-markers of alzheimer's disease via immunomagnetic reduction," *IEEE Transactions on Applied Superconductivity*, vol. 21, no. 3, pp. 477–480, 2011.
- [15] C. C. Yang, S. Y. Yang, H. H. Chen et al., "Effect of molecule-particle binding on the reduction in the mixed-frequency ac magnetic susceptibility of magnetic bio-reagents," *Journal of Applied Physics*, vol. 112, pp. 24704-1–24704-4, 2012.
- [16] W. Jiang, H. C. Yang, S. Y. Yang et al., "Preparation and properties of superparamagnetic nanoparticles with narrow size distribution and biocompatible," *Journal of Magnetism and Magnetic Materials*, vol. 283, no. 2-3, pp. 210–214, 2004.
- [17] S. Y. Yang, Z. F. Jian, H. E. Horng et al., "Dual immobilization and magnetic manipulation of magnetic nanoparticles," *Journal of Magnetism and Magnetic Materials*, vol. 320, no. 21, pp. 2688–2691, 2008.
- [18] M. C. Wergin and B. Kazer-Hotz, "Plasma vascular endothelial growth factor (VEGF) measured in seventy dogs with spontaneously occurring tumours," *In Vivo*, vol. 18, no. 1, pp. 15–20, 2004.
- [19] S. Y. Yang, W. C. Wang, C. B. Lan et al., "Magnetically enhanced high-specificity virus detection using bio-activated magnetic nanoparticles with antibodies as labeling markers," *Journal of Virological Methods*, vol. 164, no. 1-2, pp. 14–18, 2010.

